Zeitschrift: IABSE proceedings = Mémoires AIPC = IVBH Abhandlungen
Band: 12 (1988)
Heft: P-127: Experimental study of impulsive design load for rocks sheds

Artikel: Experimental study of impulsive design load for rocks sheds
Autor: Yoshida, Hiroshi / Masuya, Hiroshi / Ihara, Tomomi
DOI: https://doi.org/10.5169/seals-41129

Experimental Study of Impulsive Design Load for Rock Sheds

Etude de chocs en vue du dimensionnement de galeries de protection

Untersuchung der Impulslasten zur Bemessung von Steinschlag-Galerien

Hiroshi YOSHIDA
Prof. Dr.
Kanazawa University
Kanazawa, Japan

Hiroshi Yoshida, born 1938, received the doctoral degree from Nagoya Univ. Since 1979, he has been professor in structural mechanics Kanazawa University.

Hiroshi MASUYA
Research Instructor
Kanazawa University
Kanazawa, Japan

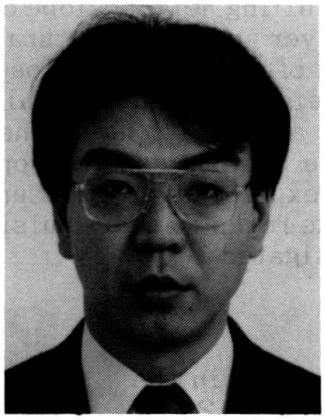

Hiroshi Masuya, born 1957, has been working at Kanazawa University since 1982. He is researching the design method for rock sheds.

Tomomi IHARA
Research Assistant
Kanazawa University
Kanazawa, Japan

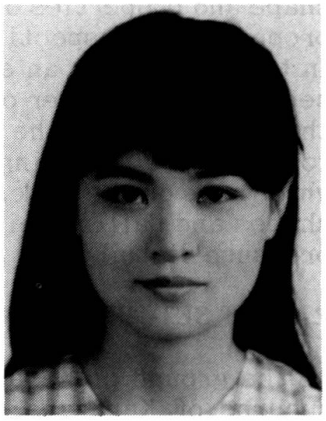

Tomomi Ihara, born 1957, has been working at Kanazawa University since 1979, She is researching the impulsive design load for rock sheds.

SUMMARY

For an estimation of the impulsive load to design rock sheds, a test set-up using a tower for the rock fall experiments was built. Using this test set-up, the impulsive accelerations of the weights simulating a falling rock and the resulting impulsive earth pressure propagating through a sand layer which acts on the rock sheds are experimentally measured. The effect of the weights, shapes and falling heights of the rocks to the impulsive acceleration and the earth pressure distribution are investigated.

RÉSUMÉ

Afin de déterminer la charge dynamique résultant de chutes de pierres, une installation a été construite avec une tour d'essais. Elle permet de mesurer l'accélération de la masse représentant la chute d'un rocher ainsi que l'onde de pression dans une couche de sable répandue sur une galerie de protection. L'étude permet aussi de mesurer l'effet de la masse, de la forme et de la hauteur de chute du rocher sur la charge dynamique et la distribution de pression dans le sol.

ZUSAMMENFASSUNG

Für die Abschätzung der Impulslasten zur Bemessung von Steinschlag-Galerien wurde eine Versuchsanlage mit einem Fallturm gebaut. Damit können zur Simulation von Felsbrocken Gewichte fallengelassen und die durch eine Sandschicht auf die Steinschlag-Galerie wirkenden Stosswellen gemessen werden. Die Einflüsse von Masse, Form und Fallhöhe auf die Stossbeschleunigung und die Erddruckverteilung wurden ebenfalls untersucht.

1. INTRODUCTION

As the Japanese island is almost covered by mountainous areas, highways were constructed along rivers on the skirts of steep mountain slopes. It is necessary to protect these highways at the most hazardous places from falling rocks by constructing structures to cover them, which are called rock sheds.
Recent Japanese main projects of road improvement intend an increase in security by decreasing the possibilities of disasters. Thus many rock sheds will be constructed in the future.
As most plans of existing rock sheds were based only on experiences at the respective site, a study based on rational theories or experimental facts is required to acquire a reasonable estimation of the impulsive load due to a rock fall and thus to give a base for the design of rock sheds/ 1- 7/.
The roof of a rock shed is usually covered by a sand layer as a shock absorbing cushion. Parameters describing the impulsive load due to a rock fall are weight, shape and properties of a rock, falling height, slope characteristics, thickness and property of a respective sand layer and the structural characteristics of rock sheds.
In this paper, for an estimation of the impulsive load to design rock sheds, a test set- up using a tower of 24. 8m height for the rock fall experiments was built. Using this test set- up, the impulsive accelerations of the weights simulating a falling rock and the resulting impulsive earth pressure propagating through a sand layer which acts on the rock sheds are experimentally measured. The effect of the weights, shapes and falling heights of the rocks to the impulsive acceleration and the earth pressure distribution are investigated.

2. TEST SET- UP AND EQUIPMENT

At the ground of Kanazawa university in the suburbs of Kanazawa city a tower of 24. 8m height was constructed to simulate a rock fall. At it' s bottom this tower was measured 7. 40m times 6. 25m and at it' s top a crane with a capacity of 50kN was set up as shown in Photo. 1. Under the tower a 20cm thick layer of pebbles was covered by a concrete slab with 0. 3m thickness and 6. 0m times 6. 0m area and above the concrete slab an open steel tank with 1. 5m height and 6. 0m times 6. 0m area filled with sand was set up.
Generally sand is used on the rock sheds as a shock absorbing cushion. The properties of the sand used in this experiment are shown in Table 1 and its particle size accumulation curve is shown in Fig. 1.
Parameters of the impulsive loads due to a rock fall are as mentioned in the introduction. However the main parameters concerning the falling rock itself are weights, shapes and falling height. In this experiment, seven weights to simulate falling rocks were used which also differed in their bottom shapes(Fig. 2). Basically circular weights of 300, 1000 and 3000kg were used. However in order to study the effect of different shapes, additionally to the sphere- bottom type, 300 and 1000kg weights with flat- and conical- bottoms were used. The weights were made by steel shells plugged with concrete so that the depth of the concrete was nearly equal to the radius of the bottom. A 20cm long cylinder was buried into

Photo. 1 Test set- up

the center of all weights to insert an accelerometer with a range up to 500g (g = gravitational acceleration).

Table 1 Properties of used sand

10% DIAMETER OF SOIL PARTICLE D_{10}(mm)	60% DIAMETER OF SOIL PARTICLE D_{60}(mm)	UNIFORMITY COEFFICIENT U_c	COEFFICIENT OF CURVATURE U
0.09	0.14	1.56	0.10

3. MEASURING DEVICES AND METHOD

3.1 Impulsive acceleration

The weight representing a falling rock was lifted up to various heights, then exposed to free fall using a special electric instrument to release it. The data sampling of the accelerations started from the instant of the collision of the weight with the sand layer and ended when the weight reached a stationary state. Accelerations in mutually perpendicular three directions were simultaneously measured taking an inclination of the weight into consideration.

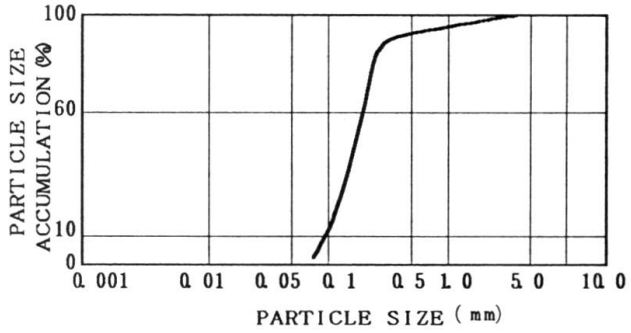

Fig. 1 Particle size accumulation curve

Amplifiers for the accelerations were placed on the top of the weight in order to avoid a loss of voltage by electric wires. These analog data of accelerations were simultaneously fed into two microcomputers for a period of two seconds, and simultaneously transformed into digital data, then recorded on cassette tapes. The acceleration waves were immediately displayed on computer display.

The transformations from analog data to digital data (A/ D transformation) were accomplished in two ways. First by the so- called low speed measurement, where the accelerations were sampled in intervals of 600Hz frequencies, and high frequency components were smoothed out passing through 200Hz low pass filters. Secondly by the high speed measurement where the accelerations are sampled in 2000Hz frequencies and without low pass filters.

3.2 Earth pressure

Either five or six earth pressure gages were set up at intervals of fifteen or thirty centimeters from the center of the sand tank bottom. These earth pressure gages were inserted into a steel board and their location was enforced by plaster to prevent lateral movement along with the sand. Data of earth pressures were fed into the microcomputer in 600Hz sampling intervals for two seconds and recorded on a cassette tape after A/ D transformation. Then wave forms of these earth pressures were displayed on computer display.

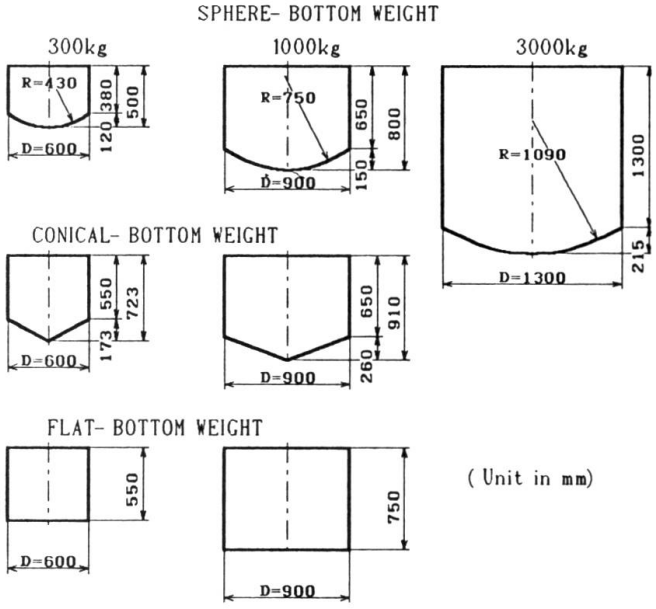

Fig. 2 Shapes and dimensions of weights

3.3 Location of the falling weight

The location of the center of the falling weight on the sand layer was measured with centimeter precision in a X–Y coordinate system set up in advance.

3.4 Weight penetrations

The distance from the bottom of a weight at it's central impact to the surface of the former undisturbed sand layer was measured as the penetration of a weight.

3.5 Water content and density

Water contents and densities of the sand layer were measured at intervals of 20cm from the bottom of sand layer to it's surface. In order to measure the density steel cylinders with 5cm radius and 5cm length were used.

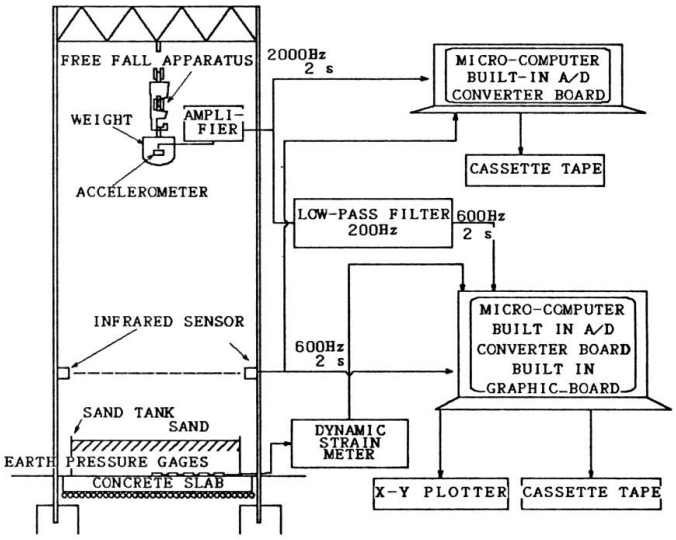

Fig. 3 Test set–up and measuring system

3.6 Cone bearing capacity

The cone bearing capacity was measured by a static penetration apparatus before and after falling as an index of the sand's stiffness in this experiment.

4. METHOD OF EXPERIMENT

In these experiments, the various kinds of weights were lifted one by one to heights of 5, 10, 15 and 20m, and then exposed to free fall into the sand filled tank. The experiments were carried out as follows:

(1) Preparation of the sand layer

The sand layer had a thickness of 90cm for the weights of 300kg and 1000kg, and 120cm for the weight of 3000kg, since additional damping effect was not to be expected for the thicknesses with more than these heights for the respective weights/4/.

The sand layer was made in the following two ways:

a) Digging a hole–method

At first a hole of about 2m radius was dug into the sand over the surface of the concrete slab and then the sand was again thrown into this hole and stiffened by foot at intervals of 20cm.

b) Throwing sand–method

After an impact of a weight, the surroundings of the hole caused by the falling weight was taken out and the sand was thrown again into the hole and stiffened by foot at intervals of twenty centimeters.

At first the experiments were done by digging a hole–method and then some experiments were undertaken by the throwing sand method.

(2) The water content, the density and the cone bearing capacity of

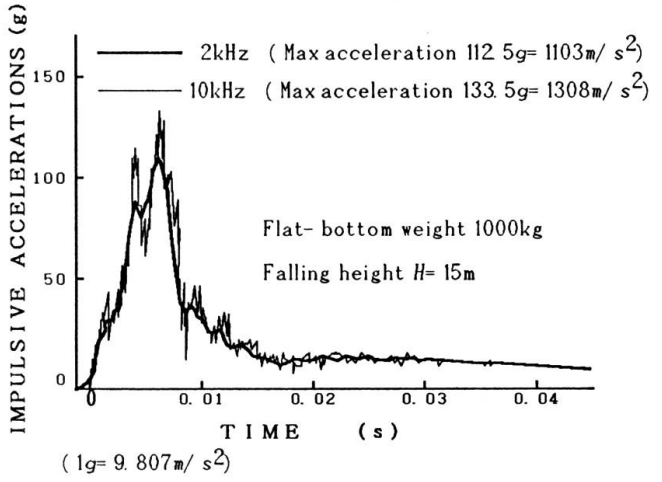

Fig. 4 Shapes of accelerations

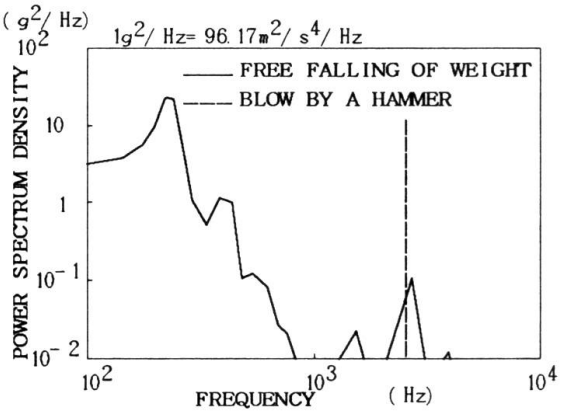

Fig. 5 Frequency analysis of the impulsive acceleration
(Flat bottom, m= 1000kg, H= 15m)

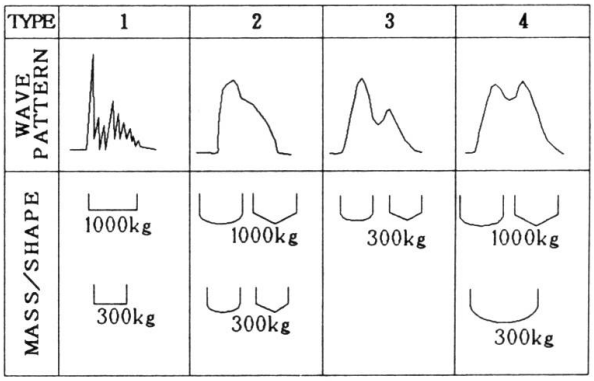

Fig. 6 Acceleration pattern

the sand layer were measured before the falling of a weight.
(3) Falling of a weight.
(4) Measurements of the impulsive accelerations (by both high speed and low speed samplings) and earth pressures. The measurement of the data by the microcomputer was activated by an infrared- ray- sensor located at a height of 3m.
(5) Mesurements of the location of a fallen weight.
(6) Measurement of the penetration into the sand.
(7) Measurements of the cone bearing capacities of the sand after the impact.

5. RESULTS OF THE EXPERIMENTS AND CONSIDERATIONS

5. 1 Wave forms of impulsive accelerations

Usually, the wave forms of impulsive accelerations are not smooth, and thus the components of high frequency waves are superimposed to components of low frequencies. Especially in the case of the flat bottom weights, this tendency is distinctly observed.
When a 1000kg weight is released from a height of 15m, two wave forms of impulsive accelerations can be differentiated according to the sampling methods shown in Fig. 4. One is the wave sampled in a 10kHz frequency, the other is the wave sampled in a 2kHz frequency through a low pass filter of 200Hz.
The result of the frequency analysis of the impulsive wave sampled in the 10kHz frequency is shown in Fig. 5. The broken line also represents the result of the frequency analysis of the impulsive wave for a blow with a hammer on the bottom of the weight. It becomes evident from Fig. 5 that the components of high frequency in the impulsive wave can be disregarded in the collision between the weight and the sand layer. As high frequency components are not of importance for this study and because they may disturb the outcome of the experiments, the sampling of the impulsive accelerations have been done in a 600Hz frequencies through 200Hz low pass filters. This measuring method will be used in the investigations of earth pressures, too.
The wave forms of impulsive accelerations are classified into 4 types(Fig. 6). Type 1, a rising and damping sawtooth like wave pattern is found in the case of the flat- bottom weights. Type 2, a monotonous wave, can be observed with sphere- and conical- bottom weights on a comparatively soft sand. Types 3 and 4 reveal wave patterns with two peaks. While type 3 is represented by sphere- and conical- bottom weights of 300kg and the first peak is higher than the second one, both peaks equal each other in type 4. Type 4 is characteristic for sphere- bottom weights of 1000kg and 3000kg as well as for conical- bottom weights of 1000kg.
As the bottom plane of the flat- bottom weight collides with the surface of the sand

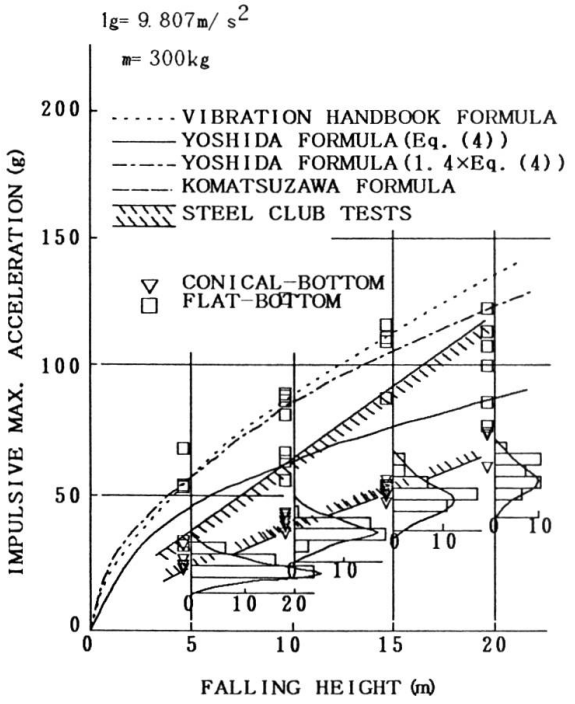

Fig. 7 Relationship between impulsive accelerations and falling heights (m= 300kg)

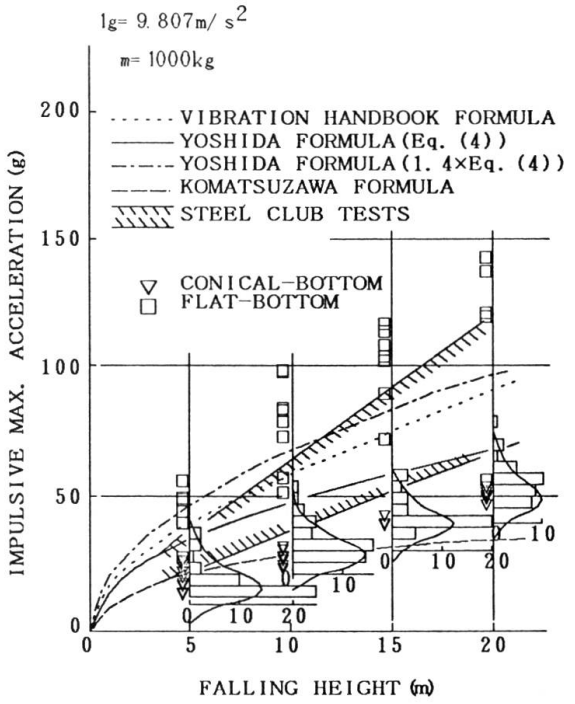

Fig. 8 Relationship between impulsive accelerations and falling heights (m= 1000kg)

layer in type 1, it is understood that a sharp sawtooth like rising and damping pattern may occur. As in type 2 the sand is comparatively soft, it can be also understood that the wave form is monotonous. But in types 3 and 4, the causes of the occurrence of two peaks and the difference between both peaks in magnitude has not yet been understood clearly.

5.2 Maximum impulsive accelerations

The relationship between maximum impulsive accelerations and falling heights concerning weights of 300kg and 1000kg is shown in Figs. 7 and 8 for three different bottom shapes. As many data of sphere-bottom weights are available, the experimental results of sphere-bottom weights are illustrated by a frequency distribution and a logarithm normal distribution, and triangle and square marks represent the experimental values of conical-bottom and flat-bottom weights in Figs. 7 and 8.

The relationship between maximum impulsive accelerations and falling heights concerning a weight of 3000kg is shown in Fig. 9. The frequency distributions show the experimental results obtained by sphere-bottom weights.

Several formulae based on simple theories of elastic statics or experimental facts in defined conditions have been proposed to represent the impulsive force by rock-falls/5, 8-12/. Some simple explanations to these equations will be provided as follows.

5.2.1 The formula of the vibration handbook for civil engineers in Japan/5/

This formula has been drawn out of Hertz's elastic contact theory on the assumption that a rigid ball runs into a half-infinite elastic ground. According to this theory, the maximum impulsive force P (kN) is given by the following equation.

$$P = 9.68\times 10^{-2}\,\lambda^{2/5} m^{2/3} H^{3/5} \qquad (1)$$

in which λ is the Lame coefficient of sand (kN/m^2), m is the mass of the falling rock

(kg) and H is the falling height (m). It is recommended in this handbook that λ is 980.7kN/m^2 for the design of rock sheds.

5.2.2 The Komatsuzawa formula/13/

This formula has been drawn out of an energy balance consideration on the assumption that the potential energy of a falling rock is equal to the energy acting on a spring representing a sand cushion. According to this theory, the maximum force is shown by the following equation.

$$P = 2.84\times 10^{-2}\, m^{5/6} k^{1/4} H^{1/2} \qquad (2)$$

in which k is the spring constant (kN/m^3) and 4903kN/m^3 is recommended for the commonly used sand.

5.2.3 Tests of the Japanese Steel Club/8/

The first experiment on the impulsive force by falling rocks was done by the socalled Japanese Steel Club. Full-scaled rock sheds were used in this experiment and the effects of a sand cushion and the structural characteristics of a rock shed on the impulsive force were investigated. It was reported that the impulsive force is given in the range between two straight lines (see Figs. 7, 8 and 9).

5.2.4 The Yoshida formula/9/

An experimental research on the impulsive force by falling weights over several kinds of sand layers on concrete foundations and prestressed concrete roofs of rock sheds was conducted by one of the authors.
This research showed that the time from the collision between a weight and a sand layer to the final stop of the weight is independent of the falling speed but depends mainly on the mass of the weight. Using maximum accelerations in the experiments, it was shown that the impulsive force was represented by the following equation.

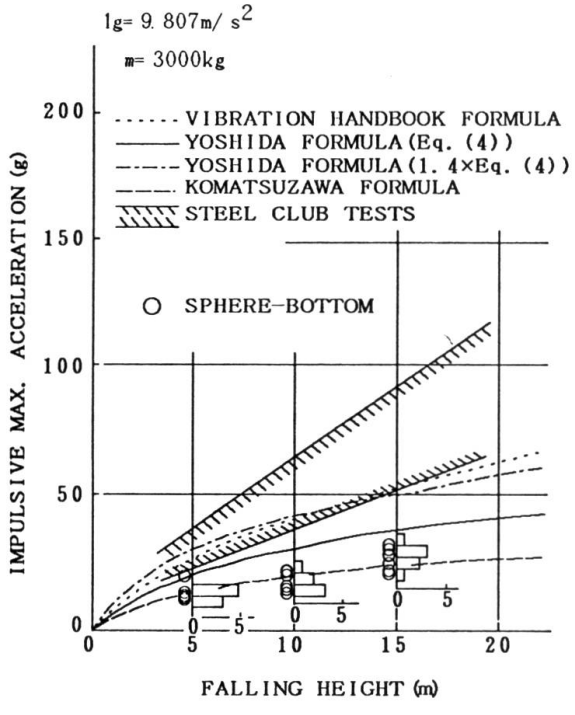

Fig. 9 Relationship between impulsive accelerations and falling heights (m= 3000kg)

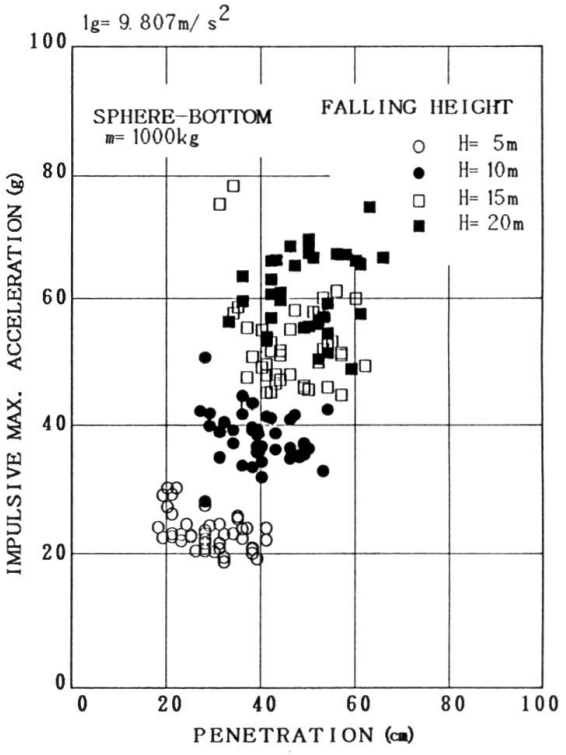

Fig. 10 Relationship between impulsive accelerations and penetrations

$$P = 2\times 10^{-3}\alpha \frac{m}{T_0}\sqrt{2gH} \qquad (3)$$

in which α is the reliability coefficient representing the confidence interval on condition of a probability, m is the mass of the rock, g is the gravity acceleration and T_0 is the time from the collision to the stop. For the sand with the properties as shown in Table 1 and Fig. 1 the impulsive force was given by the following equation with 95% reliability.

$$P = 2.42\times 10^{-3}\frac{m}{T_0}\sqrt{2gH} \qquad (4)$$

$$T_0 = 2.20\times 10^{-5}m + 0.0485\,(\mathrm{s}) \qquad (5)$$

Based on the experiment and the analysis of the dynamic response of rock sheds it is recommended to use an impact coefficient of 0.4 for the design of rock sheds.
The equational values mentioned above are shown in Figs. 7, 8 and 9. The following results became obvious after studying the relationships between the maximum impulsive accelerations and the falling heights (Figs. 7, 8 and 9).

a) The impulsive acceleration decreases with increasing weight.
b) The impulsive acceleration of sphere- and conical-bottom weights are almost equal.
c) Compared to the impulsive acceleration of sphere- and conical-bottom weights those of flat-bottom weights are remarkably greater.

5.3 The effects of the remaining parameters on the impulsive accelerations

It is expected that the crucial parameters of impulsive accelerations due to a rock fall – excluding the rock's characteristics– are thickness, properties and moisture content of a respective sand layer. By the authors past studies it became clear that the impulsive acceleration is independent on the thickness of a sand layer with more than 60cm height.

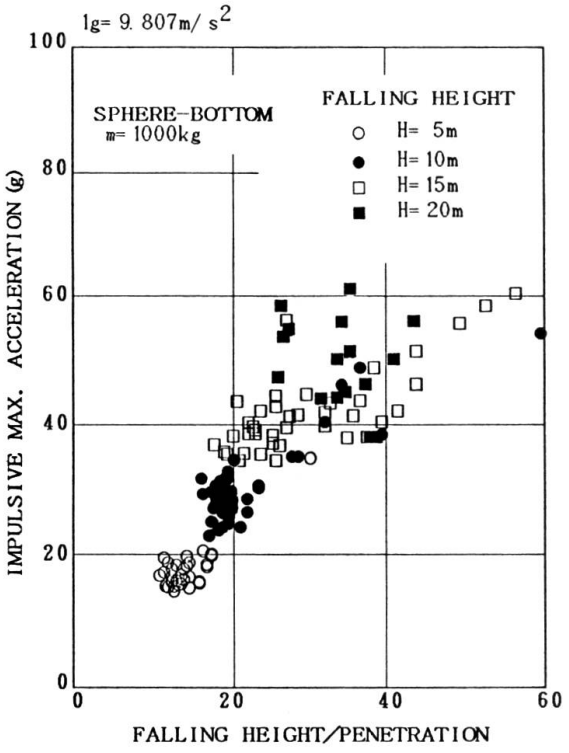

Fig. 11 Relationship between impulsive accelerations and ratios of falling height to penetration

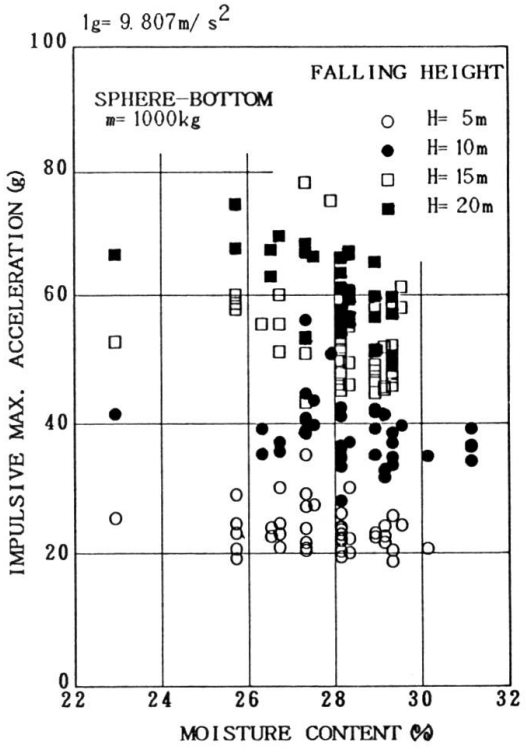

Fig. 12 Relationship between impulsive accelerations and moisture contents

Here, other relationships will be discussed: The relationship between the impulsive maximum acceleration and the ratio of the falling height to the penetration of weights; the effect of water content and the sand' s stiffness.
The effects caused by different kinds of sand layers to the impulsive acceleration are also of great importance but were not yet investigated in this study.

5. 3. 1 The relationship between the impulsive acceleration and the penetration

The case of the 1000kg sphere- bottom weight is shown in Fig. 10. For the same falling height, both acceleration and penetration show great variations. Nevertheless the accelerations have a tendency to decrease with the increase of the penetration.
Assuming that the potential energy of a weight before falling is equal to the work done by the weight penetrating the sand layer, the following equation may be introduced

$$mgH=\int_0^{T_0} P(t)\,v(t)\,dt \qquad (6)$$

in which m is the mass of the weight, g is the gravity, H is the falling height, $P(t)$ and $v(t)$ are the force applied to the sand and the velocity of the weight at time t, respectively, and T_0 is the time from the collision of a weight to it' s final stop.
Here, assuming that equation (6) is proportional to the product of a maximum impulsive force $F_{max} = ma_{max}$ by a final penetration δ, the following equation may be applied

$$a_{max} = cg\frac{H}{\delta} \qquad (7)$$

in which a_{max} is the maximum impulsive acceleration and c is a constant.
The relationship between the impulsive acceleration and the ratio of the falling height to the penetration of the weight is shown in Fig. 11. It is recognized that the impulsive acceleration is proportional to the ratio of the falling height and the

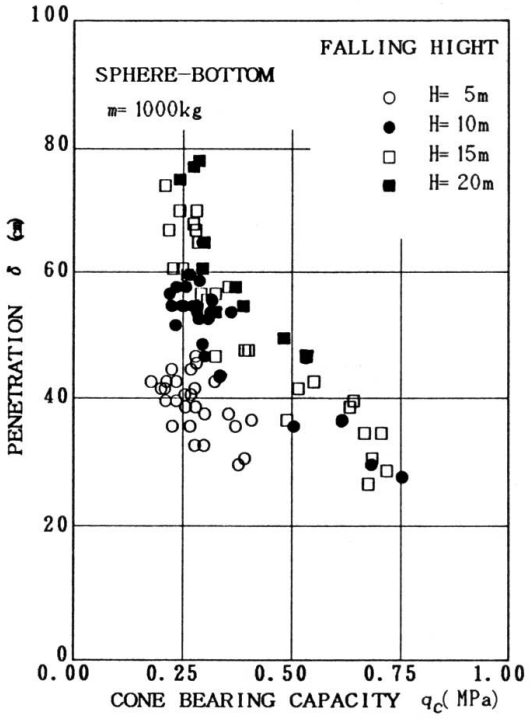

Fig. 13 Relationship between penetrations and cone bearing capacities

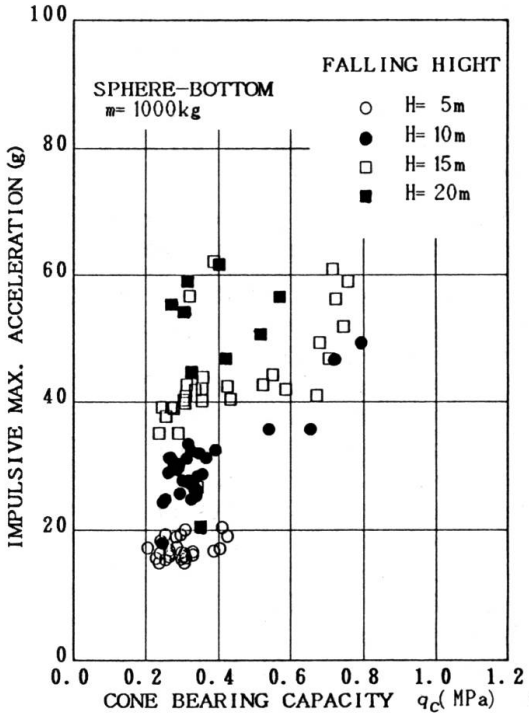

Fig. 14 Relationship between impulsive accelerations and bearing capacities

penetration of the weight. Therefore it is satisfactory to assume that equation (7) sufficiently expresses the relation between the impulsive acceleration and the penetration.

5. 3. 2 Impulsive acceleration and moisture content of sand

For the 1000kg sphere- bottom weight the relation between the impulsive acceleration and the moisture content of the sand is shown in Fig. 12. The optimum moisture content of the sand based on the compaction test is 20%. For falling heights of less than 15m, it proves that the smaller the moisture content the larger the impulsive acceleration. However in case of H = 20m, this tendency is not evident anymore.
Because of natural conditions in the field test, data below the optimal moisture content could not be obtained. A study in such a range can not be conducted.

5. 3. 3 Cone bearing capacities and accelerations

For the 1000kg sphere- bottom weight the relationship between the cone bearing capacity and the impulsive acceleration is shown in Fig. 13. The larger the cone bearing capacity the smaller the penetration and the larger the impulsive acceleration will be.
In other words, the stronger the sand's stiffness, the larger the static resistance of the cone penetration, and thus the impulsive acceleration will increase.

5. 4 Impulsive earth pressures

The considerations described above were concentrated on the impulsive accelerations of a weight. But the impulsive force encountered by rock sheds is the impulsive earth pressure acting on the bottom of the sand layer, that is to say, upon the surface of the structure's roof rather than an impulsive force acting from a weight to sand.
The following considerations are about impulsive earth pressures acting from the sand layer to the surface of a structure using the earth pressures measured on the bottom of the sand layer.

5. 4. 1 Variations in the earth pressure distribution with time

The changes in the distributions of the earth pressures with time are shown in Fig. 15(a) and(b).
For a flat- bottom weight of 1000kg and a falling height of 15m the change of the earth pressure in each location is shown in Fig. 15(a) from the moment of the collision of the weight with the sand. For a sphere- bottom weight of 1000kg and a falling height of 15m they are shown in Fig. 15(b).
For sphere- and flat- bottom weights the impulsive earth pressure wave appears 0. 015s. after the collision. It's value increases gradually and falls off relatively slowly after reaching a maximum in the case of a sphere- bottom weight.

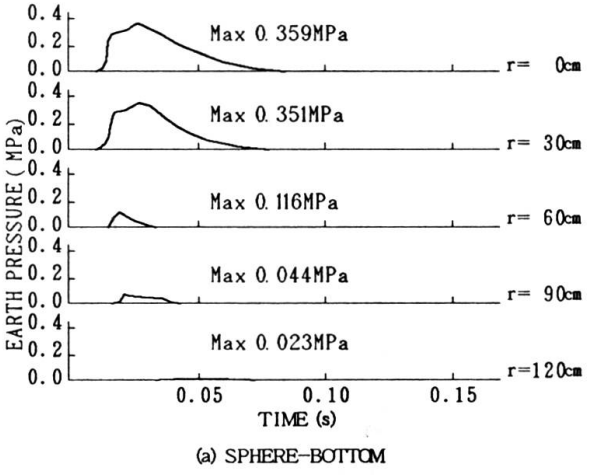

(a) SPHERE-BOTTOM

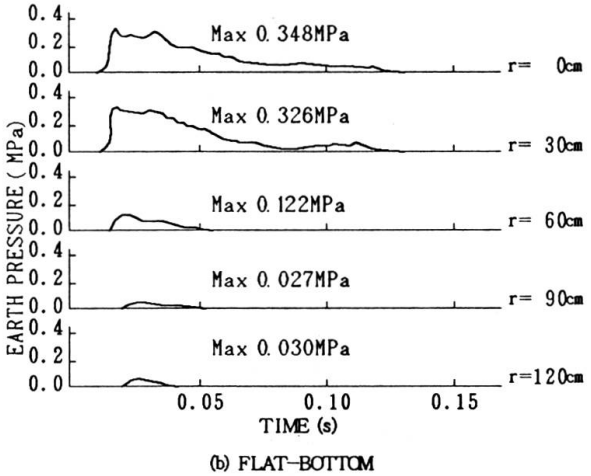

(b) FLAT-BOTTOM

Fig. 15 Earth pressures at each point

With the distance from the falling point, the delay of the earth pressure from the collision increases but it's value decreases and it's wave form becomes monotonous. The earth pressure distribution caused by a flat-bottom weight is also monotonous in spite of a rising and damping sawtooth like wave pattern of impulsive acceleration shape. In the cases of a 1000kg sphere-bottom weight with a 15m falling hight, the earth pressure distribution for both sphere- and flat-bottom weights from their impact point in radial direction measured are illustrated by Fig. 16 in an interval of 0.01s.

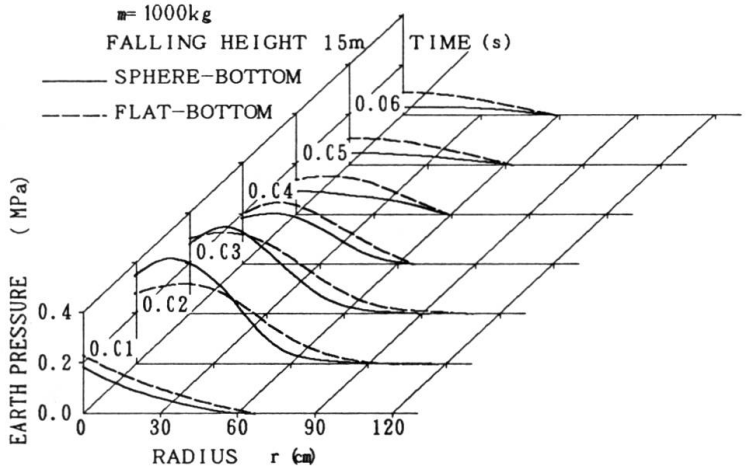

Fig. 16 Earth pressure distributions

A spline function is applied between measured points of earth pressure in this figure.

At first impulsive earth pressures appear in the neighborhood of the falling point and immediately spread radially. Then the scope of the earth pressure distribution decreases slowly.

The earth pressure caused by a flat-bottom weight is larger than that caused by sphere-bottom weights. Compared to flat-bottom weight the earth pressure caused by sphere-bottom weight are larger between 0.01s. and 0.02s. in the neighborhood of the falling point, however, in distant points this pattern is reversed.

With time both of them decrease slowly, but the earth pressure caused by a flat-bottom weight is larger than that caused by a sphere-bottom weight.

On account of the above observation it is necessary not only to consider a maximum earth pressure at each point but also changes of the earth pressure distribution with time, because the maximum earth pressure does not appear at the same time at each point.

5.4.2 Impulsive forces evaluated by accelerations of weights and by earth pressures

Assuming a symmetrical distribution of earth pressure with respect

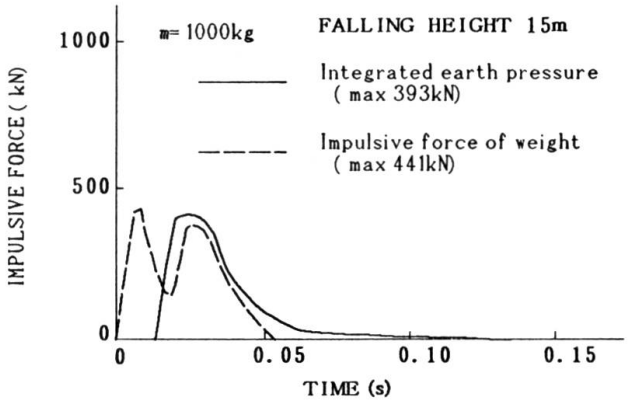

(a) SPHERE-BOTTOM

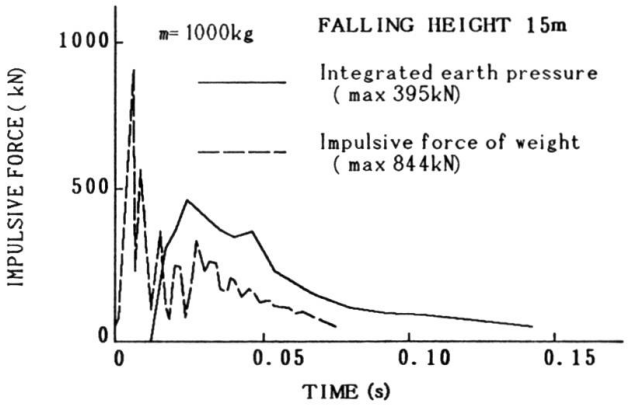

(b) FLAT-BOTTOM

Fig. 17 Impulsive load integrated earth pressure

to the axis passing through the falling point, the impulsive force $P_e(t)$ at time t evaluated by earth pressures is

$$P_e(t) = 2\pi\int_0^\infty rp(r,t)\,dr \quad (8)$$

where $p(r,t)$ is evaluated by the earth pressure in the distance r at the moment t. Because the earth pressure is negligible at a distance r= 120cm the integration of $p(r,t)$ is carried out from r= 0cm to 120cm. In the case of the sphere- bottom weight of 1000kg and a falling height of 15m, the impulsive forces evaluated by the acceleration of the weight and the earth pressure (Eq.(8)), are shown in Fig. 17(a). The latter appears 0.15s. after the collision with the weight and the maximum of the latter is a little smaller than the maximum of the former. There are two peaks in the wave of the former but the wave pattern of the latter is monotonous.

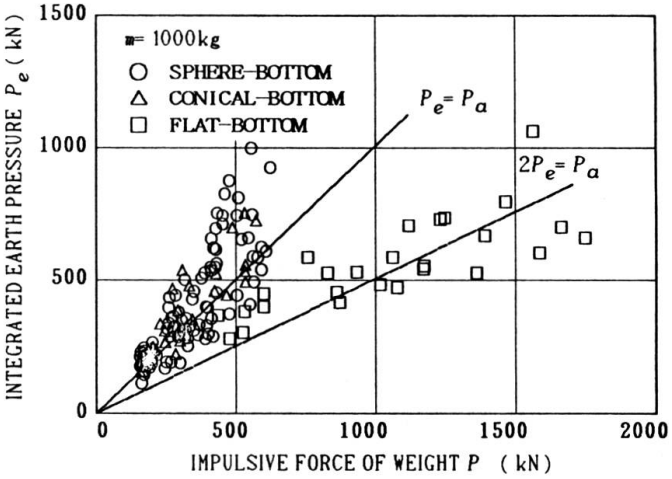

Fig. 18 Relationship between integrated earth pressures and impulsive forces of falling weight

In other cases of sphere- bottom weights, the same tendency described is found, i.e. the maximum of impulsive forces evaluated by accelerations of weights are almost equal to the integrated earth forces. In cases of conical- bottom weights, a similar description can be made. Thus there is no significant difference between sphere- and conical- bottom weights.

In case of the flat- bottom weight of 1000kg and a falling height of H= 15m, the impulsive force evaluated by the acceleration of the weight and evaluated by the earth pressure with time are shown in Fig. 17(b). Maximum forces evaluated by accelerations of flat- bottom weights are much larger than those of sphere- bottom weights as shown in Fig. 17(a) but the maximum integrated earth force is half as large as the maximum force evaluated by the acceleration of a weight and it is almost equal to the maximum integrated earth force of the sphere- bottom weights.

On account of the above observation, one can assume that the sharp peaks of the acceleration wave in flat- bottom weights are diminished during the transmission through the sand layer. The impulsive force of flat- bottom weights evaluated by the earth pressure distribution diminishes after its maximum slower than the one of flat- weights.

Fig. 18 represents the relationship between the integrated earth pressures and the impulsive forces of the 1000kg weight. The impulsive forces of sphere- and conical-

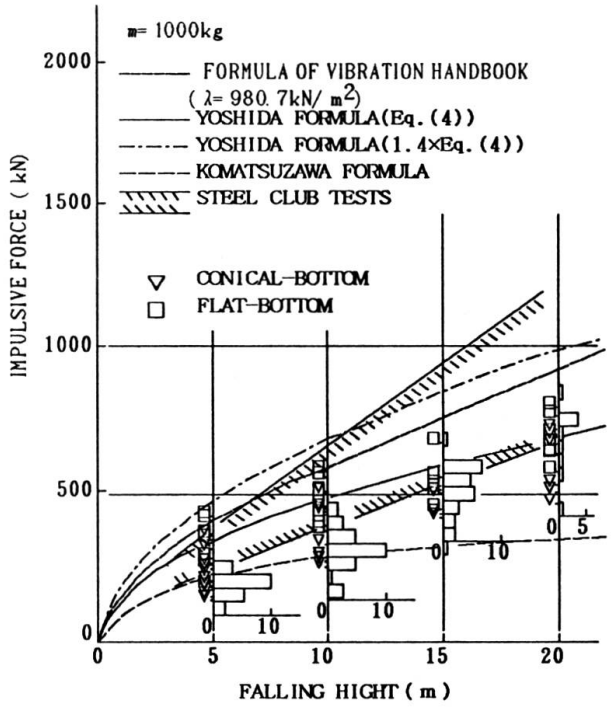

Fig. 19 Relationship between integrated earth pressures and falling heights

bottom weights, evaluated by maximum accelerations are almost equal to the maximum of the integrated earth forces, that is to say, the impacting forces upon rock sheds. But in case of flat-bottom weights, the integrated earth forces are roughly half as large as those evaluated by maximum accelerations
Comparing each of the 1000kg weights in concern of the relationship between the integrated earth pressures and the falling heights, it is found that the integrated forces by flat-bottom weights are slightly larger than those of the other weights, and that the impacting forces to the rock sheds are not so depending on the shapes of the weights.

6. CONCLUSIONS AND DESIGN RECOMMENDATIONS

The following conclusions can be drawn based upon the above investigations.
(1) The waves of impulsive accelerations of sphere- and conical-bottom weights are relatively monotonous. But waves of impulsive accelerations of flat-bottom weights appear in a sharp-toothed edge pattern.
(2) The impulsive forces evaluated by maximum accelerations of sphere-bottom weights are almost equal to those of conical-bottom weights compared to the far larger ones of flat-bottom weights.
(3) The larger the mass of a weight the smaller it's impulsive acceleration.
(4) The impulsive acceleration of a weight is almost proportional to the ratio of the falling height to the penetration.
(5) In case of stiffened sand with a large cone bearing capacity the penetration of a weight is small and the impulsive force is large.
(6) Components of high frequencies in impulsive forces are diminished through sand. In case of sphere- and conical-bottom weights, earth pressures are strongly distributed in the immediate neighborhood of the falling point, contrary to flat-bottom weights with a relatively wide spread distribution around the falling point. Also the sharp peek is not apparent as measured acceleration.
(7) In case of sphere- and flat-bottom weights, the maximum integrated earth force is almost equal to the impulsive force evaluated by the maximum acceleration of a weight.
(8) In case of flat-bottom weights, the maximum integrated earth forces are half as large as the impulsive forces evaluated by the accelerations of a weight.
(9) If maximum integrated earth forces are considered to be forces acting upon rock sheds, Yoshida's formula almost approximates the upper limit of the maximum in all experimental data.
(10) Waves of integrated earth forces differ with the shapes of the weights. The dynamic effects to rock sheds due to these differences are unknown and offer a vast field for future investigations.
The design of rock sheds should take into consideration the following
(1) Design impulsive force acting on the roof of rock sheds due to rock falls can be evaluated by Equations (3) in which the duration of impulsive force is considered.
(2) Thicknesses of 90cm for rocks less than 1000kg and 120cm for those less than 3000kg are enough for a sand layer.
(3) The effect of the shapes of falling rocks on the impulsive force can be negligible.

REFERENCES

1. EXPRESS HIGHWAY RESEARCH FOUNDATION OF JAPAN: The Research Report of Preventative Structures Against Rock Falls (in Japanese), Feb. 1974.
2. JAPAN ROAD ASSOCIATION: The Research Report of Preventative Structures on Roads (in Japanese), Mar. 1980.
3. JAPAN RAILWAY CIVIL ENGINEERING ASSOCIATION: Manual for Preventative Structures Against Rock Falls (in Japanese), Mar. 1978.
4. JAPAN ROAD ASSOCIATION: Handbook of Preventations Against Rock Falls (in Japanese), Mar. 1978.

5. JAPAN SOCIETY OF CIVIL ENGINEERS: Vibration Handbook for Civil Engineers (in Japanese), 1966, pp. 320–324.
6. PFISTER, F.: Die Steinschlaggalerien on der Axenstrasse, Schweizerishe Bauzeitung, 90 Jahrgang, Heft 44, Oct. 1972, pp. 1118–1120.
7. RÖSLI, A.: The Dynamic Behaviour of Prestressed Bridges, IABSE, Sixth Congress, Stockholm, June, 1960.
8. JAPAN STEEL CLUB: Study on Development of a New Type Rock Shed (in Japanese), Apr. 1973.
9. YOSHIDA, H., ISHIZUKA, K., and HOSOKAWA, Y.: Experimental Study on the Estimation of Impulsive Load for Preventative Structures Against Rock Falls (in Japanese), 13th meeting of Japan Road Association, Oct. 1976, pp. 35–41.
10. MINISTRY OF CONSTRUCTION CIVIL ENGINEERING RESEARCH INSTITUTE: The Research Report of Impulsive Load due to Rock Falls on a Sand Layer (in Japanese), Research Materials, No. 1822, Mar. 1982.
11. SONODA, K., KOBAYASHI, T. and SUZUKI, T.: An Estimation of Load due to a Rock Fall on Rock Sheds (in Japanese), The Report of 1st Symposium on Impulsive Load due to a Rock Falls and Design of Rock Sheds, Edited by H. Yoshida, July 1983, pp. 25–35.
12. YOSHIDA, H. et al.: Impulsive Load due to Rock Falls on a Sand Cusion and Spread of Load (in Japanese), The Report of 1st Symposium on Impulsive Load due to Rock Falls and Design of Rock Sheds, Edited by H. Yoshida, July 1983, pp. 1–8.
13. KAZUHITO, T. and AKAZAWA, M.: Railway Construction (in Japanese), 1963, pp. 263–272.